Pair Density Distribution Function of Membrane Particles at Low Density

Dear Sir:

It is shown that the leading edge of the pair density distribution function (PDDF) of visible particles in membranes contains information about their size and shape at the plane of contact. This can be used to test theories of membrane structure.

PDDFs have been used for many years as convenient devices for describing the distributions of particles that are observed in freeze fracture electron micrographs of biological membranes (1–3). They are also the necessary output of Monte Carlo simulations (4, 5) that attempt to model the distributions seen in micrographs. The major features of a typical PDDF are the location and shape of the leading edge, and the locations and shapes of subsequent peaks and troughs. The principal purpose of Monte Carlo modeling is to produce a PDDF that matches, as closely as possible, the measured PDDF of a micrograph, and so to deduce from the model information about the possible size, shape, and interactions of the observed particles.

The majority of Monte Carlo calculations are carried out with the interaction energy dependent solely on the separation of the centers of the particles (e.g., 6). This implies that the particles may be treated as spheres or circles, although for liquid crystals, ellipsoids have been considered (7). In electron micrographs of biological membranes, the apparent shape of the particles may include artifacts generated by the freeze fracture process and also by the shadowing. However, the particles often appear to be not circularly symmetrical and it has been found that the leading edge of the PDDF is neither a vertical line (as required by circles) nor a curve that can be represented by a simple analytical function. Because of the complexity of the leading edge, it has been largely ignored and attention has been focussed on the major peaks.

This paper shows that in principle, complete information about the size and shape of the particles in their plane of contact is contained in the leading edge of the PDDF if the particles are hard and at low density. The word "hard" is used in both senses: not distorted by contact with a neighbor, and having no knowledge of the existence of a neighbor until contact is made. The density is assumed to be low enough that two-particle collisions dominate.

The leading edge of the PDDF is generated by contact between nearest neighbors, i.e., when there is steric hindrance. For the sake of simplicity and illustration, we consider the particles to have only two dimensions and to be rectangular (Fig. 1). Assume rectangle R_1 is fixed in a plane and rectangle R_2 is free to move around it in the same plane. At any position of R_2, defined by r and θ, $\beta_1(r, \theta) + \beta_2(r, \theta)$ represents the range of angles through which R_2 can rotate without overlapping R_1.

The probability function $P(r)$ of any non–overlapping configuration with R_2 at a distance r from R_1 is:

$$P(r) = \tfrac{1}{2}\pi \int_0^{2\pi} (\beta_1(r, \theta) + \beta_2(r, \theta))/\pi \, d\theta \qquad (1)$$

i.e., $P(r)$ depends only on the angular degrees of freedom available to R_2.

From Fig. 1 it can be seen that the lower limit to $P(r)$ occurs

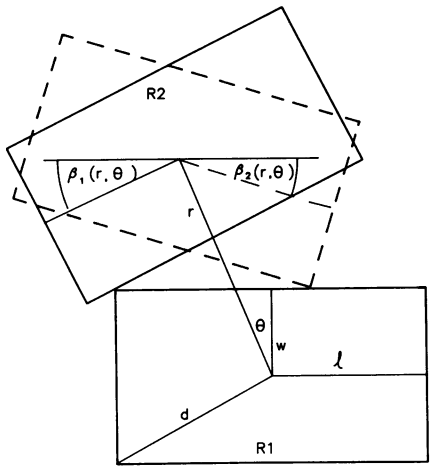

FIGURE 1 Rectangles R_1 and R_2 showing the range of angles $\beta_1(r, \theta)$ and $\beta_2(r, \theta)$ through which R_2 can rotate when its center is given by r and θ with respect to the center of R_1.

where $r < 2W$, in which case $\beta_1(r, \theta) + \beta_2(r, \theta) = 0$ for all θ, so $P(r) = 0$. The upper limit is when $r > 2d$, making $\beta_1(r, \theta) + \beta_2(r, \theta) = \pi$ for all θ so $P(r) = 1$ as expected.

For two identical rectangles, the angles $\beta_1(r, \theta)$ and $\beta_2(r, \theta)$ are simple to calculate for each value of r and θ, although the calculations can become tedious. In Fig. 1, once $r > \ell + w$, there are angles additional to $\beta_1(r, \theta) + \beta_2(r, \theta)$ for which the rectangles do not overlap. For shapes other than rectangles the calculation of the overlap angles is not necessarily a trivial matter.

Equation 1 can be solved analytically for many simple shapes or can be solved numerically. For more complicated shapes, $P(r)$ can be evaluated using Monte Carlo techniques. Fig. 2 shows $P(r)$ as a function of r for rectangles with ℓ:w = 3:2 together with the pair density distribution function $g(r)$ derived from a Monte Carlo simulation of 56 such particles at a density of 0.01 after 10^8 trial moves. The only difference between the curves is the slight noise on $g(r)$. Examples of curves of $P(r)$-vs.-r for squares, 75°

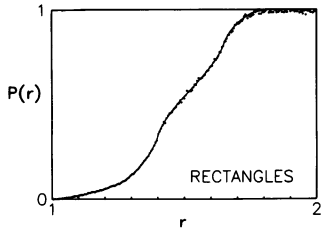

FIGURE 2 (*Solid line*) probability $P(r)$ of finding rectangle R_2 at a center–center distance r from rectangle R_1. r is normalized with respect to the distance of closest approach. Both rectangles have ℓ:w = 3:2. (*Dots*) Pair density distribution function $g(r)$-vs.-normalized r derived from a Monte Carlo simulation of 56 rectangles ℓ:w = 3:2, density = 0.01, number of trial moves = 10^8.

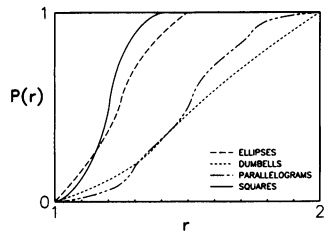

FIGURE 3 $P(r)$-vs.-normalized r calculated from Eq. 1 for squares, 75° parallelograms ℓ:w = 3:2, ellipses ℓ:w = 3:2 and "dumbells" (two discs joined at a common point).

parallelograms (ℓ:w = 3:2), ellipses (ℓ:w = 3:2), and "dumbells" (two discs joined at a common point) are shown in Fig. 3.

Published PDDFs of intramembranous particles do not have vertical leading edges. Simulation, using models based on hard discs, will always give a vertical leading edge (4). The limitation imposed by small sample sizes and the consequent choice of boxes for histograms can affect the apparent shape of the PDDF. When the width of the boxes is not small compared with the width of the peaks, the peaks are flattened and the leading edge is spread out. The sharply rising leading edge for hard discs can be spread over two boxes unless the position of the box edge is adjusted to coincide with the nearest possible approach distance. The useable sample size can be increased by using methods that allow counts over separate areas to be combined (8).

Pearson et al. (4) have suggested two explanations for the slope of the leading edge of PDDFs. If the particles deform as soft discs or if they have a range of sizes, then the leading edge would not be vertical. Monte Carlo simulations of models based on these two suggestions show that either the particles must deform by up to 50% of their radii or a random distribution of sizes over the range of 2:1 is required. It is because these requirements are improbable that an explanation based on particle shape is suggested.

We have attempted to fit the PDDFs for distributions of particles in human erythrocyte membranes published by Pearson et al. (Fig. 4 of ref. 4). The curves for group I can be fitted, Fig. 4, by a model based on hard elliptical particles with a ratio of long to short axes of 1.75:1 at the observed particle number density (4,100/μm^2). The constraints imposed by number density prevent

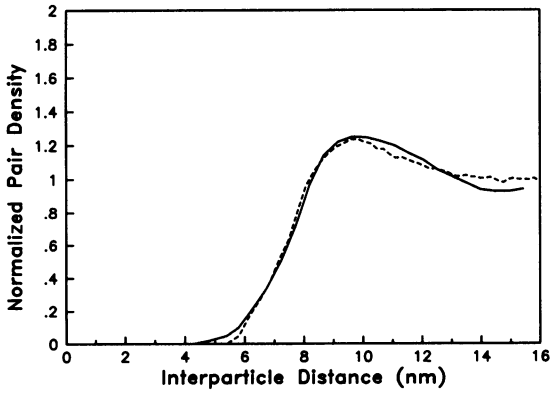

FIGURE 4 Averaged PDDF for distribution of human erythrocyte membrane (continuous line) taken from group I from Pearson, Hui, and Stewart (4) compared with PDDF from model using ellipses with a long-to-short axis ratio of 1.75:1 (11 nm × 6.2 nm) (dashed line).

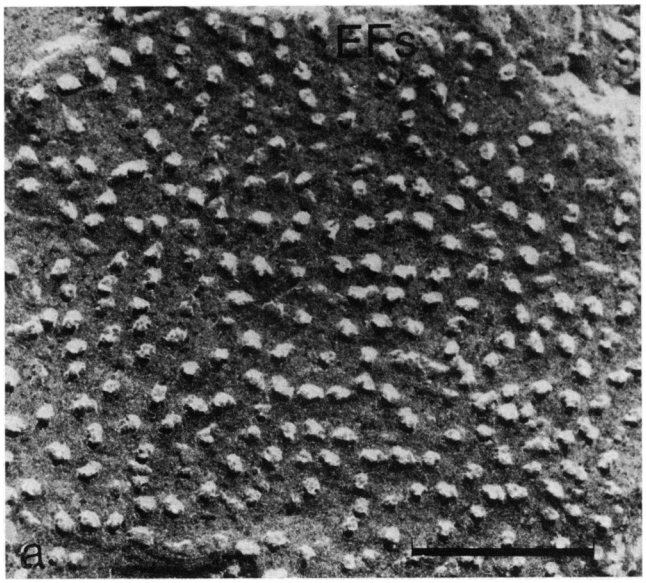

FIGURE 5 Electron micrograph of freeze-fractured membrane of barley mutant. Bar, 125 nm (kindly supplied by D. J. Simpson).

matching of the curves for groups II and III because the size of the model particles needed to raise the packing density to match the height of the peaks in the observed PDDFs moves the position of the peak to higher interparticle distances.

As a further example, the PDDF for the particles revealed by freeze fracture electron micrographs of a barley mutant, Fig. 5, is shown as a histogram in Fig. 6. It was not found possible to fit this histogram by any of the simple shapes of hard particles, but a good fit (continuous line in Fig. 6) was obtained by assuming the particles were hard ellipses with the observed point offset from the center of the ellipse.

One would speculate from Fig. 3 that each particle shape leads to a unique shape for the leading edge of the PDDF. An examination of Eq. 1 shows that this is likely to be true. The angles $\beta_1(r, \theta)$ and $\beta_2(r, \theta)$ are very sensitive to particle shape and depend in a complex way on r. For $P(r)$ for one shape to be the same as $P(r)$ for a different shape, for all values of r, would require an enormous number of numerical coincidences. In our opinion this is so unlikely that we conclude that each particle

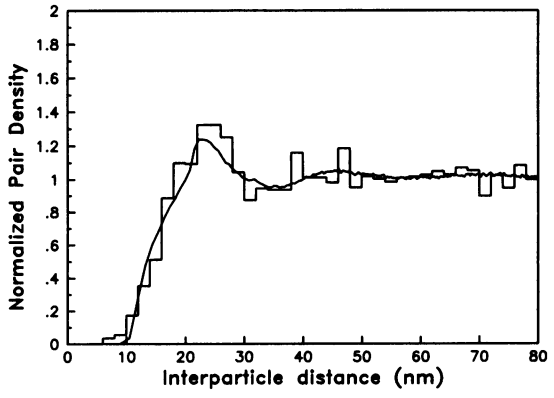

FIGURE 6 PDDF of particles from Fig. 5 (histogram) compared with PDDF of ellipses 21.4 nm × 17.8 nm with the observed point offset 5.2 nm from center along the long axis (continuous curve).

shape generates its own unique leading edge to the PDDF, i.e., the leading edge contains all the information about the size and shape of the particles.

For the shapes discussed above, third particle interactions start to distort the form of the leading edge at a density of ~0.3; and at a density of 0.5, identification of the shape can be difficult. However, for the many electron micrographs of membranes in which the particle density is low, an indication of the particle shape can be derived by studying the leading edge of the PDDF. The shape revealed in this way is not necessarily the shape seen in the electron micrograph. Since the PDDF depends on the shape of the particles in their plane of contact, this simply means that the plane of contact is not necessarily the fracture plane viewed in the micrograph.

Clearly, a comparison of the leading edge of the measured PDDF with $P(r)$ calculated from Eq. 1 represents a powerful test of any theory of membrane structure that proposes that the visible particles within the membrane have specific shapes. However, the preciseness of any conclusion is governed by uncertainties in the measured PDDFs arising from the limited resolution of freeze fracture electron micrographs, the small number of particles and experimental artifacts.

J. MIDDLEHURST AND N. S. PARKER
CSIRO, *Division of Food Research, North Ryde, NSW 2113, Australia*

Received 31 December 1985 and in final form 9 June 1986.

REFERENCES

1. Mehlhorn, R. J., and L. Packer. 1976. Analysis of freeze-fracture electron micrographs by a computer-based technique. *Biophys. J.* 16:613–625.
2. Donnell, J. T., and L. X. Finegold. 1981. Testing of aggregation measurement techniques for intramembranous particles. *Biophys. J.* 35:783–798.
3. Goodchild, D. J., J. T. Duniec, and J. M. Anderson. 1983. The lateral displacement of intramembranous particles in chloroplast membranes as a function of light intensity. FEBS (*Fed. Eur. Biochem. Soc.*) Lett. 154:243–246.
4. Pearson, R. P., S. W. Hui, and T. P. Stewart. 1979. Correlative statistical analysis and computer modelling of intramembranous particles distributions in human erythrocyte membranes. *Biochim. Biophys. Acta.* 557:265–282.
5. Cornell, B. A., J. Middlehurst, and N. S. Parker. 1981. Modelling the simplest form of order in biological membranes. *J. Colloid Interface Sci.* 81:280–282.
6. Abraham, F. F. 1981. The phases of two-dimensional matter, their transitions, and solid-state stability: a perspective via computer simulation of simple atomic systems. *Phys. Reports.* 80:340–374.
7. Perram, J. W. 1985. Statistical mechanics of hard ellipsoids I. Overlap algorithm and the contact function. *J. Comput. Phys.* 58:409–416.
8. Duniec, J. T., D. J. Goodchild, and S. W. Thorne. 1982. A method of estimating radial distribution function of protein particles in membranes from freeze fracture electron micrographs. *Comput. Biol. Med.* 12:319–322.